organic compounds

Hydrogen-bonded supramolecular motifs in pyrimethaminium 4-methylbenzoate, pyrimethaminium 3-hydroxypicolinate and pyrimethaminium 2,4-dichlorobenzoate

Kaliyaperumal Thanigaimani and Packianathan Thomas Muthiah*

School of Chemistry, Bharathidasan University, Tiruchirappalli 620 024, Tamilnadu, India
Correspondence e-mail: tommtrichy@yahoo.co.in

In 2,4-diamino-5-(4-chlorophenyl)-6-ethylpyrimidin-1-ium (pyrimethaminium, PMNH) 4-methylbenzoate, $C_{12}H_{14}ClN_4^+ \cdot C_8H_7O_2^-$, (I), pyrimethaminium 3-hydroxypicolinate, $C_{12}H_{14}ClN_4^+ \cdot C_6H_4NO_3^-$, (II), and pyrimethaminium 2,4-dichlorobenzoate, $C_{12}H_{14}ClN_4^+ \cdot C_7H_3Cl_2O_2^-$, (III), the PMNH cations interact with the carboxylate groups of the corresponding anion via nearly parallel N—H···O hydrogen bonds, forming $R_2^2(8)$ ring motifs. A description of the observed arrays of quadruple hydrogen bonds in (I) and (II) in terms of hydrogen donors and acceptors (the DA model), their graph-set motifs and the resulting supramolecular ladder is given. In (III), supramolecular chains along the b axis and helical chains along the a axis are formed via N—H···O hydrogen bonds involving the 2-amino and 4-amino groups of the PMNH cation, respectively. Weak Cl···Cl interactions are also found in (III).

Comment

Pyrimethamine (PMN) is an antifolate drug used in the treatment of malaria. In the chemotherapy of malaria and neoplastic diseases, substituted 2,4-diaminopyrimidines are widely employed as metabolic inhibitors of pathways leading to the synthesis of proteins and nucleic acids (Hitchings & Burchall, 1965). PMN acts against malarial parasites by selectively inhibiting their dihydrofolate reductase–thymidylate synthase (Sardarian et al., 2003). PMN is also used along with other drugs for the treatment of opportunistic infections in patients suffering from AIDS (Tanaka et al., 2004). 2-Aminopyrimidine and its derivatives form good adducts as they readily form hydrogen-bonded patterns through their stereochemically associated amine group and ring N atom (Lynch et al., 2000). The crystal structures of PMN (Sethu-

raman & Thomas Muthiah, 2002) and many of its salts have been reported from our laboratory (Sethuraman et al., 2003; Stanley et al., 2005). The present study of the title salts, pyrimethaminium 4-methylbenzoate, (I), pyrimethaminium 3-hydroxypicolinate, (II), and pyrimethaminium 2,4-dichlorobenzoate, (III), was undertaken to obtain more information regarding patterns of hydrogen bonding in these types of compounds.
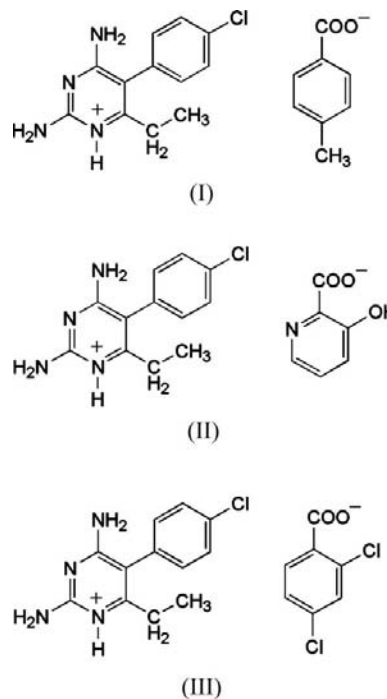
Views of compounds (I)–(III) are shown in Figs. 1–3 and comparative geometric parameters are given in Table 1. In these compounds, the asymmetric unit contains one pyrimethaminium cation, together with a 4-methylbenzoate anion in (I), a 3-hydroxypicolinate anion in (II) and a 2,4-dichlorobenzoate anion in (III). As expected, in all three crystal structures the PMNH cations are protonated at the N1 position. The dihedral angle between the 2,4-diaminopyrimidine and 4-chlorophenyl planes is 80.11 (14)° in (I), 68.28 (9)° in (II) and 72.50 (8)° in (III). These values are close to those
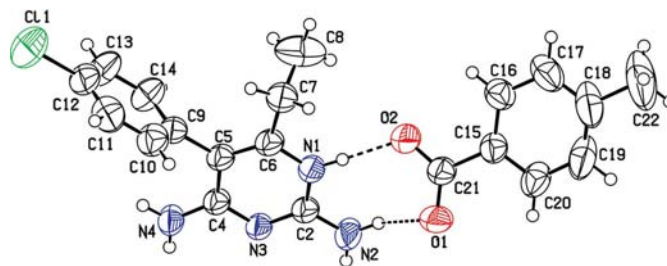

Figure 1
The asymmetric unit of (I), showing the atom-numbering scheme. Displacement ellipsoids are drawn at the 50% probability level and H atoms are shown as small spheres of arbitrary radii. Dashed lines indicate hydrogen bonds.

Figure 2
The asymmetric unit of (II), showing the atom-numbering scheme. Displacement ellipsoids are drawn at the 50% probability level and H atoms are shown as small spheres of arbitrary radii. Dashed lines indicate hydrogen bonds.
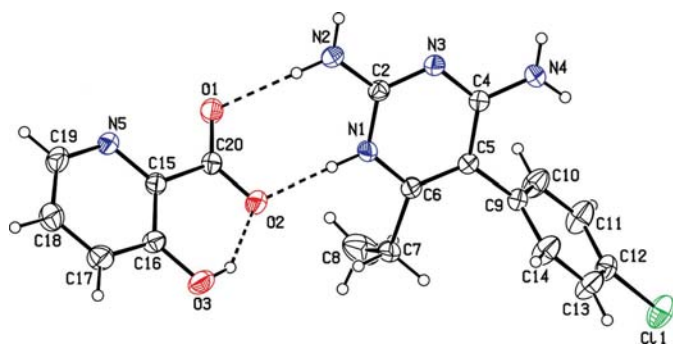

Figure 3
The asymmetric unit of (III), showing the atom-numbering scheme. Displacement ellipsoids are drawn at the 50% probability level and H atoms are shown as small spheres of arbitrary radii. Dashed lines indicate hydrogen bonds.
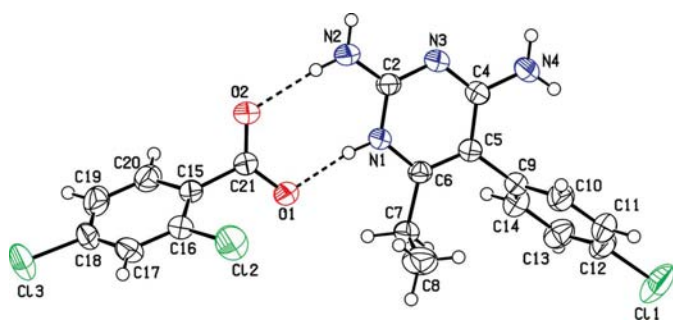

Figure 4
A view of the *DADA* and *DDAA* arrays of hydrogen bonds leading to a supramolecular ladder in (I). Dashed lines indicate hydrogen bonds and H atoms not involved in hydrogen bonding have been omitted. [Symmetry codes: (i) $-x + 1$, y, $-z + \frac{3}{2}$; (ii) $-x + \frac{1}{2}$, $-y + \frac{1}{2}$, $-z + 1$; (iii) $x - \frac{1}{2}$, $-y + \frac{1}{2}$, $z - \frac{1}{2}$.]

Figure 5
The crystal structure of (II). Dashed lines indicate hydrogen bonds and H atoms not involved in hydrogen bonding have been omitted. [Symmetry codes: (i) $-x + 2$, $-y + 1$, $-z + 1$; (ii) $-x + 2$, $y + \frac{1}{2}$, $-z + \frac{3}{2}$.]

observed in modelling studies of dihydrofolate reductase pyrimethamine (DHFR–PMN) complexes (Sansom *et al.*, 1989). Such modelling studies of DHFR–PMN complexes indicate that this dihedral angle is important for the proper docking of the drug molecule at the active site of the enzyme (Sansom *et al.*, 1989). By contrast, the value of the C5—C6—C7—C8 torsion angle (Table 1), representing the twist of the ethyl group from the pyrimidine ring plane, is not very important, as it does not affect the overall binding energy of the enzyme–drug complex (Sansom *et al.*, 1989).

In each of (I)–(III), the carboxylate group of the respective anion (4-methylbenzoate, 3-hydroxypicolinate and 2,4-dichlorobenzoate, respectively) interacts with the protonated pyrimidine moiety of PMNH through a pair of nearly linear N—H···O hydrogen bonds, to form an eight-membered $R_2^2(8)$ ring motif (Etter, 1990; Bernstein *et al.*, 1995) (Figs. 1–3). This motif has been observed in modelling studies of DHFR–PMN complexes (Sansom *et al.*, 1989), and it is one of the 24 most frequently observed motifs in organic crystal structures (Allen *et al.*, 1998).

In (I), the $R_2^2(8)$ motifs are crosslinked *via* N—H···O hydrogen bonds to produce a *DDAA* array (where *D* is a hydrogen-bond donor and *A* is a hydrogen-bond acceptor) of quadruple hydrogen bonds (Table 1); this can be represented by the graph-set notations $R_2^2(8)$ and $R_4^2(8)$ (see Fig. 4). The inversion-centre-related PMNH cations are also base-paired
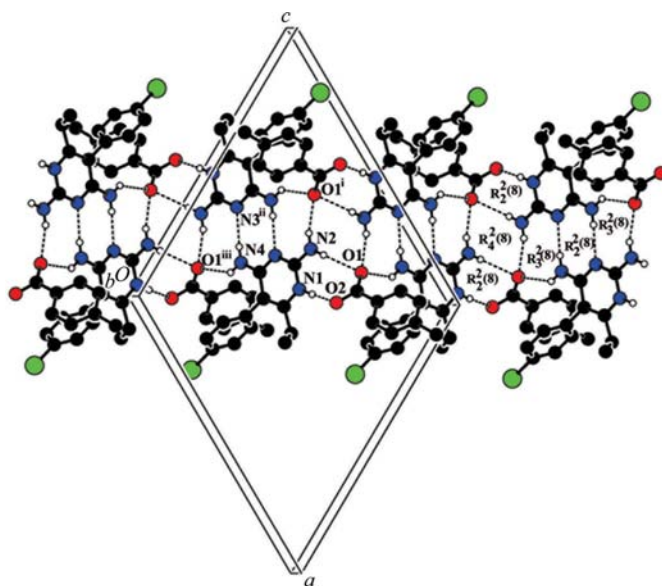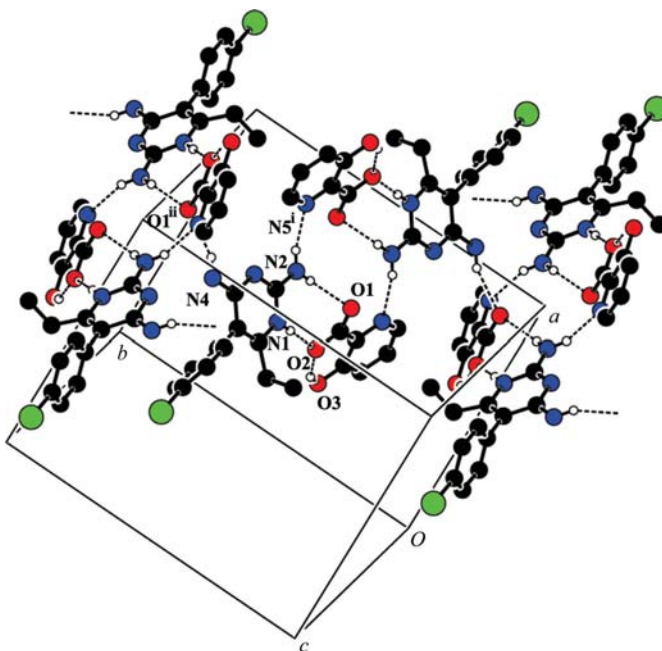
via N—H···N hydrogen bonds involving the unprotonated pyrimidine N atom and the 4-amino group (Table 2). This type of base pairing, also with an $R_2^2(8)$ motif, has been observed in many diaminopyrimidinecarboxylate salts (Stanley *et al.*, 2005). In addition to the base pairing, a hydrogen-bonded acceptor (O1) bridges the 4-amino and 2-amino groups on the sides of the pairing, leading to a complementary linear *DADA*
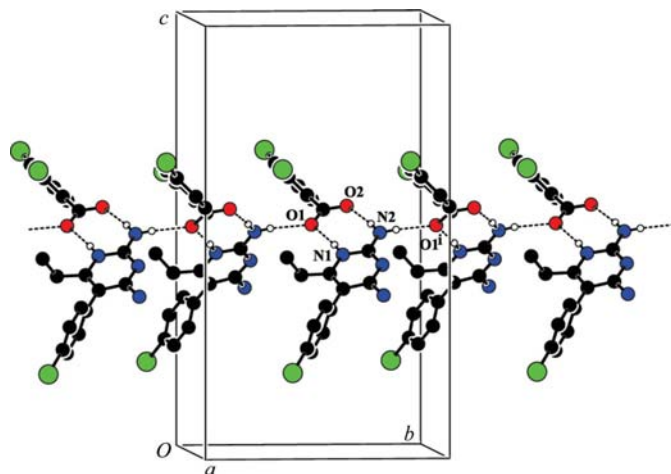
organic compounds

Figure 6
N—H···O hydrogen-bonding patterns in the supramolecular chain of (III). Dashed lines indicate hydrogen bonds and H atoms not involved in hydrogen bonding have been omitted. [Symmetry code: (i) $-x + \frac{3}{2}$, $y + \frac{1}{2}$, z.]

array of quadruple hydrogen bonds with rings having graph-set notation $R_2^2(8)$ and $R_3^2(8)$. In general, only one of the motifs (*DADA* or *DDAA* array) has been identified at any one time in diaminopyrimidinecarboxylate salts. Here, both the *DADA* and *DDAA* array motifs co-exist in an alternating manner to form a hydrogen-bonded supramolecular ladder (Fig. 4). The *DDAA* array and the *DADA* array are approximately perpendicular to one another (Stanley *et al.*, 2005).

In (II) (Table 3), inversion-related molecules (binary motifs) are connected *via* N—H···N hydrogen bonds to form an array with an $R_4^4(14)$ ring motif. This array is futher crosslinked *via* N—H···O hydrogen bonds (Fig. 5). A typical intramolecular hydrogen bond exists between the hydroxy and carboxylate groups of the 3-hydroxypicolinate anion to form a six-membered hydrogen-bonded ring [$S(6)$, Fig. 2].

In (III), the 2-amino group of the PMNH cation interacts with one of the carboxylate O atoms (O1) through an N—H···O hydrogen bond, to form supramolecular chain motifs $C_2^1(6)$ and $C_2^2(6)$ along the *b* axis (Fig. 6). In addition, the 4-amino group of the PMNH cation interacts with one of the carboxylate O atoms (O2) through an N—H···O hydrogen bond, to form a zigzag chain along the *a* axis (Fig. 7) with motif $C_2^1(8)$. N1—H1···O1 hydrogen bonds are also involved in these patterns. Details of these hydrogen bonds are given in Table 4. Further, the cations and anions are linked by weak Cl···Cl interactions (Table 5) which are not observed in compounds (I) and (II).

In conclusion, in all three crystal stuctures the PMNH cation interacts with the carboxylate O atoms *via* N—H···O hydrogen bonds to form the frequently observed hydrogen-bonded eight-membered $R_2^2(8)$ ring motif. In compound (I), the $R_2^2(8)$ motifs are further bridged by N—H···O hydrogen bonds on either side, forming a *DDAA* array of quadruple hydrogen bonds. In (I), N—H···N base pairing is observed, while there is none in compounds (II) and (III). In (I), both *DADA* and *DDAA* array motifs co-exist in an alternating manner to form a hydrogen-bonded supramolecular ladder.
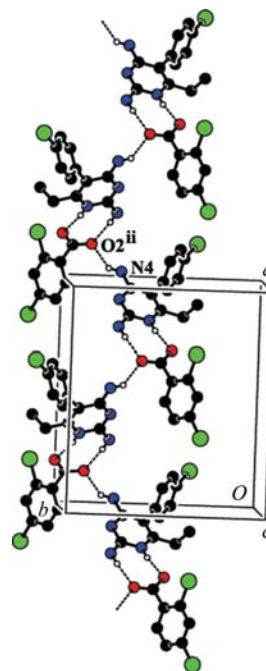

Figure 7
View of the N—H···O hydrogen bonds responsible for the zigzag chain of hydrogen bonding in (III). Dashed lines indicate hydrogen bonds and H atoms not involved in hydrogen bonding have been omitted. [Symmetry code: (ii) $x + \frac{1}{2}$, $-y + \frac{3}{2}$, $-z + 1$.]

Thus, it appears that the variation in supramolecular organization depends in part on the nature of the side chain attached to the anionic ring, *viz*. 4-methylbenzoate, 3-hydroxypicolinate or 2,4-dichlorobenzoate.

Experimental

Compounds (I)–(III) were prepared by mixing hot methanol solutions (20 ml) of pyrimethamine (62 mg; Shah Pharma Chemicals, India) with hot aqueous solutions (40 ml) of the corresponding acid [4-methylbenzoic acid (34 mg, Loba Chemie) for (I), 3-hydroxypicolinic acid (34 mg, Loba Chemie) for (II) and 2,4-dichlorobenzoic acid (47 mg, Loba Chemie) for (III)] in a 1:1 molar ratio, and warming for 30 min on a water bath. Each solution was cooled slowly and kept at room temperature. After a few days, colourless crystals were obtained in each case.

Compound (I)

Crystal data

$C_{12}H_{14}ClN_4^+ \cdot C_8H_7O_2^-$	$V = 4099.77\,(13)$ Å^3
$M_r = 384.86$	$Z = 8$
Monoclinic, $C2/c$	Mo $K\alpha$ radiation
$a = 17.1373\,(3)$ Å	$\mu = 0.21$ mm^{-1}
$b = 16.4776\,(3)$ Å	$T = 293$ K
$c = 16.6127\,(3)$ Å	$0.15 \times 0.12 \times 0.12$ mm
$\beta = 119.080\,(1)°$	

Data collection

Bruker SMART APEXII CCD area-detector diffractometer	32486 measured reflections
Absorption correction: multi-scan (*SADABS*; Bruker, 2008)	3398 independent reflections
$T_{min} = 0.970$, $T_{max} = 0.975$	2474 reflections with $I > 2\sigma(I)$
	$R_{int} = 0.038$

Table 1
Selected geometric parameters in (I), (II) and (III) (Å, °).

	(I)	(II)	(III)
Cl1—C12	1.739 (3)	1.7347 (19)	1.735 (2)
N1—C2	1.345 (4)	1.360 (2)	1.356 (2)
N1—C6	1.360 (3)	1.363 (2)	1.368 (2)
N3—C2	1.323 (3)	1.325 (2)	1.329 (2)
N3—C4	1.342 (3)	1.338 (2)	1.336 (2)
C5—C9	1.485 (3)	1.492 (2)	1.486 (2)
C2—N1—C6	120.9 (2)	121.03 (13)	121.14 (14)
C2—N3—C4	117.5 (2)	117.61 (14)	117.51 (14)
C5—C6—C7—C8	−102.6 (3)	−88.4 (2)	88.1 (2)

Table 2
Hydrogen-bond geometry (Å, °) for (I).

D—H$\cdots A$	D—H	H$\cdots A$	$D\cdots A$	D—H$\cdots A$
N1—H1$\cdots$O2	0.86	1.73	2.586 (3)	173
N2—H2$A\cdots$O1^i	0.86	2.14	2.947 (3)	157
N2—H2$B\cdots$O1	0.86	2.23	2.988 (3)	147
N4—H4$A\cdots$N3^{ii}	0.86	2.14	2.996 (3)	176
N4—H4$B\cdots$O1^{iii}	0.86	2.36	3.043 (3)	136

Symmetry codes: (i) $-x + 1, y, -z + \frac{3}{2}$; (ii) $-x + \frac{1}{2}, -y + \frac{1}{2}, -z + 1$; (iii) $x - \frac{1}{2}, -y + \frac{1}{2}, z - \frac{1}{2}$.

Table 3
Hydrogen-bond geometry (Å, °) for (II).

D—H$\cdots A$	D—H	H$\cdots A$	$D\cdots A$	D—H$\cdots A$
N1—H1$\cdots$O2	0.86	1.88	2.7370 (18)	175
N2—H2$A\cdots$N5^i	0.86	2.15	2.948 (2)	154
N2—H2$B\cdots$O1	0.86	2.08	2.8873 (19)	157
O3—H3$\cdots$O2	0.82	1.82	2.5462 (19)	146
N4—H4$A\cdots$O1^{ii}	0.86	2.17	2.982 (2)	158

Symmetry codes: (i) $-x + 2, -y + 1, -z + 1$; (ii) $-x + 2, y + \frac{1}{2}, -z + \frac{3}{2}$.

Refinement

$R[F^2 > 2\sigma(F^2)] = 0.047$	247 parameters
$wR(F^2) = 0.144$	H-atom parameters constrained
$S = 1.04$	$\Delta\rho_{max} = 0.42$ e Å^{-3}
3398 reflections	$\Delta\rho_{min} = -0.39$ e Å^{-3}

Compound (II)

Crystal data

C$_{12}$H$_{14}$ClN$_4^+$·C$_6$H$_4$NO$_3^-$	$V = 1856.89$ (9) Å^3
$M_r = 387.82$	$Z = 4$
Monoclinic, $P2_1/c$	Mo $K\alpha$ radiation
$a = 11.2563$ (3) Å	$\mu = 0.24$ mm^{-1}
$b = 14.3968$ (4) Å	$T = 293$ K
$c = 11.7902$ (3) Å	$0.22 \times 0.20 \times 0.18$ mm
$\beta = 103.625$ (1)°	

Data collection

Bruker SMART APEXII CCD area detector diffractometer	21858 measured reflections
	5622 independent reflections
Absorption correction: multi-scan (SADABS; Bruker, 2008)	3927 reflections with $I > 2\sigma(I)$
$T_{min} = 0.950$, $T_{max} = 0.959$	$R_{int} = 0.028$

Table 4
Hydrogen-bond geometry (Å, °) for (III).

D—H$\cdots A$	D—H	H$\cdots A$	$D\cdots A$	D—H$\cdots A$
N1—H1$\cdots$O1	0.86	1.88	2.7321 (19)	171
N2—H2$A\cdots$O1^i	0.86	2.14	2.964 (2)	159
N2—H2$B\cdots$O2	0.86	2.00	2.857 (2)	174
N4—H4$A\cdots$O2^{ii}	0.86	2.14	2.866 (2)	141

Symmetry codes: (i) $-x + \frac{3}{2}, y + \frac{1}{2}, z$; (ii) $x + \frac{1}{2}, -y + \frac{3}{2}, -z + 1$.

Table 5
Cl$\cdots$Cl interactions (Å, °) in (III).

X—$I\cdots J$	I—J	X—$I\cdots J$
C12—Cl1$\cdots$Cl3^i	3.1969 (11)	140.52 (8)
C18—Cl3$\cdots$Cl1^{ii}	3.1969 (11)	152.35 (10)

Symmetry codes: (i) $1 + x, \frac{1}{2} - y, -\frac{1}{2} + z$; (ii) $-1 + x, \frac{1}{2} - y, \frac{1}{2} + z$.

Refinement

$R[F^2 > 2\sigma(F^2)] = 0.051$	246 parameters
$wR(F^2) = 0.153$	H-atom parameters constrained
$S = 1.05$	$\Delta\rho_{max} = 0.39$ e Å^{-3}
5622 reflections	$\Delta\rho_{min} = -0.35$ e Å^{-3}

Compound (III)

Crystal data

C$_{12}$H$_{14}$ClN$_4^+$·C$_7$H$_3$Cl$_2$O$_2^-$	$V = 4084.96$ (10) Å^3
$M_r = 439.72$	$Z = 8$
Orthorhombic, $Pbca$	Mo $K\alpha$ radiation
$a = 14.3808$ (2) Å	$\mu = 0.47$ mm^{-1}
$b = 12.6799$ (2) Å	$T = 293$ K
$c = 22.4021$ (3) Å	$0.25 \times 0.22 \times 0.20$ mm

Data collection

Bruker SMART APEXII CCD area-detector diffractometer	26496 measured reflections
	5639 independent reflections
Absorption correction: multi-scan (SADABS; Bruker, 2008)	3791 reflections with $I > 2\sigma(I)$
$T_{min} = 0.891$, $T_{max} = 0.912$	$R_{int} = 0.033$

Refinement

$R[F^2 > 2\sigma(F^2)] = 0.042$	255 parameters
$wR(F^2) = 0.118$	H-atom parameters constrained
$S = 1.01$	$\Delta\rho_{max} = 0.48$ e Å^{-3}
5639 reflections	$\Delta\rho_{min} = -0.51$ e Å^{-3}

All H atoms were positioned geometrically and refined using a riding model, with C—H = 0.93–0.97 Å and N—H = 0.86 Å in (I)–(III), and O—H = 0.82 Å in (II), and with U_{iso}(H) = $1.5U_{eq}$(C,O) for OH groups in (II) and for all methyl groups, and U_{iso}(H) = $1.2U_{eq}$(C,N) for all other H atoms.

For all three compounds, data collection: *APEX2* (Bruker, 2008); cell refinement: *SAINT* (Bruker, 2008); data reduction: *SAINT*; program(s) used to solve structure: *SHELXS97* (Sheldrick, 2008); program(s) used to refine structure: *SHELXL97* (Sheldrick, 2008); molecular graphics: *PLATON* (Spek, 2009); software used to prepare material for publication: *PLATON*.

organic compounds

References

Allen, F. H., Raithby, P. R., Shields, G. P. & Taylor, R. (1998). *Chem. Commun.* pp. 1043–1044.

Bernstein, J., Davis, R. E., Shimoni, L. & Chang, N.-L. (1995). *Angew. Chem. Int. Ed. Engl.* **34**, 1555–1573.

Bruker (2008). *APEX2, SAINT* and *SADABS*. Bruker AXS Inc., Madison, Wisconsin, USA.

Etter, M. C. (1990). *Acc. Chem. Res.* **23**, 120–126.

Hitchings, G. H. & Burchall, J. J. (1965). *Advances in Enzymology*, Vol. 27, edited by F. Nord, p. 417. New York: Interscience.

Lynch, D. E., Singh, M. & Parsons, S. (2000). *Cryst. Eng.* **3**, 71–79.

Sansom, C. E., Schwalbe, C. H., Lambert, P. A., Griffin, R. J. & Stevens, M. F. G. (1989). *Biochim. Biophys. Acta*, **995**, 21–27.

Sardarian, A., Douglas, K. T., Read, M., Sims, P. F. G., Hyde, J. E., Chitnumsub, P., Sirawaraporn, R. & Sirawaraporn, W. (2003). *Org. Biomol. Chem.* **1**, 960–964.

Sethuraman, V., Stanley, N., Muthiah, P. T., Sheldrick, W. S., Winter, M., Luger, P. & Weber, M. (2003). *Cryst. Growth Des.* **3**, 823–828.

Sethuraman, V. & Thomas Muthiah, P. (2002). *Acta Cryst.* E**58**, o817–o818.

Sheldrick, G. M. (2008). *Acta Cryst.* A**64**, 112–122.

Spek, A. L. (2009). *Acta Cryst.* D**65**, 148–155.

Stanley, N., Muthiah, P. T., Geib, S. J., Luger, P., Weber, M. & Messerschmidt, M. (2005). *Tetrahedron*, **61**, 7201–7210.

Tanaka, R., Arai, T. & Hirayama, N. (2004). *Anal. Sci. X-ray Struct. Anal. Online*, **20**, x175–x176.